A Low-Complexity Graph-Based LMMSE Receiver for MIMO ISI Channels with M-QAM Modulation

Pınar Şen Electrical and Computer Engineering
University of California, San Diego
San Diego, California
Email: psen@eng.ucsd.edu
A. Özgür Yılmaz Electrical and Electronics Engineering
Middle East Technical University
Ankara, Turkey
Email: aoyilmaz@metu.edu.tr

arXiv:1405.3057v2 [cs.IT] 1 May 2015

Abstract

In this paper, we propose a low complexity graph-based linear minimum mean square error (LMMSE) equalizer in order to remove inter-symbol and inter-stream interference in multiple input multiple output (MIMO) communication. The proposed state space representation inflicted on the graph provides linearly increasing computational complexity with block length. Also, owing to the Gaussian assumption used in the presented cycle-free factor graph, the complexity of the suggested equalizer structure is not affected by the size of the signalling space. In addition, we introduce an efficient way of computing extrinsic bit log-likelihood ratio (LLR) values for LMMSE estimation compatible with higher order alphabets which is shown to perform better than the other methods in the literature. Overall, we provide an efficient receiver structure reaching high data rates in frequency selective MIMO systems whose performance is shown to be very close to a genie-aided matched filter bound through extensive simulations.

Keywords

Gaussian assumption, Gaussian message passing, factor graph, turbo decoding, MIMO ISI channel, linear LMMSE equalization, extrinsic LLR computation.

I. INTRODUCTION

MIMO systems have attracted much attention in recent years since they potentially provide high spectral efficiency in wireless communication applications. Yet, they require complicated receiver structures so as to handle the distortion caused by the wireless channel characteristics such as the intersymbol interference (ISI) resulting from the frequency selectivity of the channel between each transmit and receive antenna pair.

In recent studies, low complexity equalizer structures are proposed to mitigate those distorting effects in MIMO ISI channels. Although, frequency domain (FD) approaches hold an important place in the literature [1], [1], [2], [2]–[4], due to the problems related to FD methods, low complexity time domain approaches have drawn interest from the perspective of the lately studied factor graph theory [5]–[10]. Belief propagation and sum product algorithms on factor graphs were proposed for both single input single output (SISO) and MIMO systems [11], [12], but they have $O(M^{\tilde{P}})$ complexity per symbol where M is the constellation size and $\tilde{P}$ is the total number of *non-zero* interferers.

The Guassian assumption utilized in the equalizer structures which provides constant complexity with increasing alphabet size has become popular lately. As an example, Kalman filtering was proposed for coded frequency selective MIMO systems in [13]. However, it has $O(P^3)$ complexity per symbol where P is the number of interferers, and more importantly lacks the improvement that backward recursion provides. On the other hand, the Gaussian message passing (GMP) rules including Kalman filtering (forward recursion) and Kalman smoothing (backward recursion) operations are derived [7], [9] and used in the implementation of LMMSE equalization on factor graphs. This approach has the advantage of complexity linearly increasing with block length N as compared to conventional block LMMSE filter's $O(N^3)$ complexity [14]. Although the factor graph structures with cycles using the GMP rules were proposed for SISO and MIMO

ISI channels respectively in [15], [16], our main focus is the cycle free ones due to exact equivalence to LMMSE filtering avoiding any iterations. There are two different cycle free factor graph structure presented in the literature for SISO systems [10], [17]. The generalization of [10] to MIMO ISI channels was proposed in [18] which still has $O(P^3)$ complexity per symbol. In addition, the mentioned studies including the GMP rules do not have any performance results for modulation types other than BPSK signaling due to the lack of LLR exchange algorithm.

In this study, however, we reduce the complexity to $O(P^2)$ per symbol with the help of a factor graph structure which takes its roots from [17]. Moreover, using Gaussian approximation of GMP rules keeps the complexity of the graph algorithm constant with the increasing constellation size. In addition, the presented approach here brings the ease of involving existing *a priori* information of the transmitted symbols, hence perfectly matched with the turbo concept for coded systems. It is also well suited to fast fading environments since the channel taps (possibly time-varying) are directly included in the graph. Therefore, the proposed structure is a very advantageous way of implementing LMMSE filtering for equalization of MIMO ISI channels.

Another important contribution of this study is the proposed LLR exhange algorithm for M-QAM signaling. LMMSE equalizers involved in turbo decoders need a method for transition to binary domain, i.e., bit LLR domain. In the literature, there were effective approaches to obtain bit LLRs from the LMMSE equalizer outputs, such as the Wang-Poor (WP) approach [19], [20] and the Joint Gaussian (JG) approach [21]. However, applying the WP or JG approaches directly is computationally intensive for factor graphs. Although a simplified expression for extrinsic LLR computation was proposed in [17] for BPSK signaling only, there is no such a work for higher order constellations in the literature within the knowledge of the authors except the heuristic methods in [22], [23]. To fill up this gap, we derive a transformation from the graph outputs to the bit LLRs based on the WP approach for higher order modulation alphabets. Owing to this key connection, extrinsic bit LLR values can be obtained in accordance with the graph solution without major complexity increase.

In summary, two main contributions of this study can be listed as

- a state space graph for time domain LMMSE equalization of MIMO ISI channels with a

reduced complexity as compared to the techniques in the literature,

- a computationally simple method to obtain extrinsic bit LLRs from LMMSE equalizer outputs for M-QAM signaling in both SISO and MIMO systems.

Overall, the performance of the proposed extrinsic bit LLR producing algorithm is shown to be better as compared to the heuristic methods in the literature for M-QAM signaling. Also, the performance of the extended LMMSE equalizer using this LLR producing algorithm is shown to be very close to a hypothetical genie-aided matched filter bound [24] through extensive simulations which makes it an efficient receiver that can reach high data rates in frequency selective MIMO systems.

The paper is organized as follows. Section II gives the system model. Section III presents our proposed factor graph-based LMMSE equalizer design. In Section IV, the proposed LLR exchange algorithm is analyzed in details. We discuss the computational complexity of the suggested receiver in Section V. Section VI presents the bit error rate (BER) performance results of the proposed receiver structure. Lastly, Section VII concludes the paper.

II. SYSTEM MODEL

The notations used in the paper are organized as follows. Lower case letters (e.g., x) denote scalars, lower case bold letters (e.g., $\mathbf{x}$) denote vectors, upper case bold letters (e.g., $\mathbf{X}$) denote matrices. For a given random variable x; m_x, v_x, w_x and $w_x m_x$ denote its mean, variance, weight and weighted mean values respectively where $w_x \triangleq v_x^{-1}$. For a given vector random variable $\mathbf{x}$; $\mathbf{R_x}, \mathbf{m_x}, \mathbf{V_x}, \mathbf{W_x}$ and $\mathbf{W_x m_x}$ denote its autocorrelation matrix, mean vector, covariance matrix, weight matrix and weighted mean vector respectively where $\mathbf{W_x} \triangleq \mathbf{V_x}^{-1}$. The indicators $()^*$, $()^H$, and $E\{\}$ denote conjugate, Hermitian transpose and expectation operations respectively and $\mathbf{I}$ denotes the identity matrix of proper size. The operation $diag\{\mathbf{A}\}$ is defined as the diagonal elements of a matrix $\mathbf{A}$.

We consider a MIMO single-carrier communication system which suffers from the ISI effect due to the wireless nature of the channel. The block diagram of the discussed transmitter and receiver structures are depicted in Figure 1. At the transmitter side, after the coded information

bits are interleaved and modulated according to an M-QAM alphabet S, modulated symbols are spread to N_t transmit antennas and sent over the ISI channel which occurs between each transmit and receive antenna. At the receiver side, a turbo structure including the proposed graph based LMMSE equalizer and *a posteriori* probability (APP) decoder is operated by use of observations coming from N_r receive antennas.

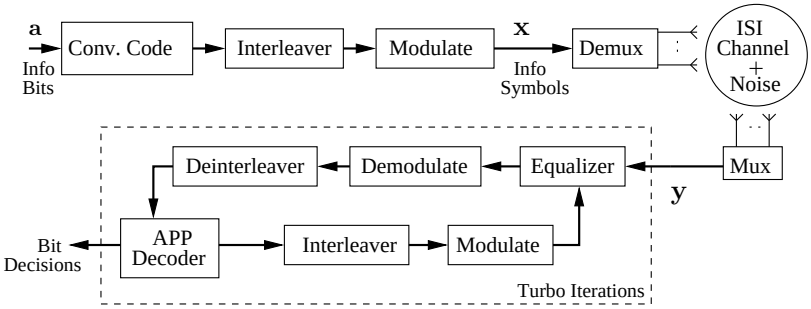

Fig. 1: System Model

We can model the given discrete-time system at time k as

$$\mathbf{y}_k = \sum_{i=0}^{L-1} \mathbf{H}_i \mathbf{x}_{k-i} + \mathbf{n}_k \,; \quad k = 1, 2, \ldots, N + L - 1, \tag{1}$$

$$\mathbf{H}_i = \begin{bmatrix} h_{11}(i) & h_{12}(i) & \ldots & h_{1N_t}(i) \\ h_{21}(i) & h_{22}(i) & \ldots & h_{2N_t}(i) \\ \vdots & \vdots & \vdots & \vdots \\ h_{N_r1}(i) & h_{N_r2}(i) & \ldots & h_{N_rN_t}(i) \end{bmatrix}_{N_r \times N_t} ; \tag{2}$$

where L is the number of channel taps; N is the transmission block length; $\mathbf{H}_i$ is the $N_r \times N_t$ channel matrix at time i; $\mathbf{x}_k$ is the transmitted symbol vector of size N_t at time k; $\mathbf{y}_k$ is the observation vector of size N_r at time k and $\mathbf{n}_k$ represents additive white circularly symmetric complex Gaussian noise vector with zero mean and covariance $N_0\mathbf{I}_{N_r}$ at time k, i.e., $\mathbf{n}_k \sim CN(0, N_0\mathbf{I}_{N_r})$. The input symbol sequence is assumed to include independent, identically distributed (i.i.d.) random variables and the transmitted symbol vector $\mathbf{x}_k$ at time k is

$$\mathbf{x}_k = [x_{k,1}\ x_{k,2}\ \ldots\ x_{k,N_t}]^T \quad k = 1, 2, \ldots N \tag{3}$$

where $x_{k,l}$ is the symbol transmitted at the l^{th} transmit antenna at time k and its average energy is defined as E_s, i.e., $E\{|x_{k,l}|^2\} \triangleq E_s$. For notational convenience, we define $J \triangleq L-1$ which denotes the memory of the channel.

The matrix representation of (1) could be written as below by combining all observations with the help of multiplexing operation in Figure 1

$$\mathbf{y} = \mathbf{H}\mathbf{x} + \mathbf{n}, \quad \text{where} \tag{4}$$

$$\mathbf{y} = \begin{bmatrix} \mathbf{y}_1 \\ \mathbf{y}_2 \\ \vdots \\ \mathbf{y}_{N+J} \end{bmatrix}_{N_r(N+J)\times 1}, \ \mathbf{n} = \begin{bmatrix} \mathbf{n}_1 \\ \mathbf{n}_2 \\ \vdots \\ \mathbf{n}_{N+J} \end{bmatrix}_{N_r(N+J)\times 1}, \tag{5}$$

$$\mathbf{H} = \begin{bmatrix} \mathbf{H}_0 & \mathbf{0} & \dots & \dots & \dots & \mathbf{0} \\ \mathbf{H}_1 & \mathbf{H}_0 & \ddots & & & \vdots \\ \vdots & & \ddots & \ddots & & \vdots \\ \mathbf{H}_J & \dots & & \mathbf{H}_0 & \ddots & \vdots \\ \mathbf{0} & \ddots & & & \ddots & \mathbf{0} \\ \vdots & \ddots & \mathbf{H}_J & & & \mathbf{H}_0 \\ \vdots & & \ddots & \ddots & & \vdots \\ \vdots & & & \ddots & \mathbf{H}_J & \mathbf{H}_{J-1} \\ \\ \mathbf{0} & \dots & \dots & \dots & \mathbf{0} & \mathbf{H}_J \end{bmatrix}_{N_r(N+J)\times N_t N}, \ \mathbf{x} = \begin{bmatrix} \mathbf{x}_1 \\ \mathbf{x}_2 \\ \vdots \\ \mathbf{x}_N \end{bmatrix}_{N_t N\times 1} \tag{6}$$

For the described system model, the details of the proposed equalizer structure are given in the subsequent section.

III. GRAPH BASED LMMSE EQUALIZER FOR MIMO ISI CHANNEL

In this section, we elucidate the proposed graph structure together with the message passing algorithm. The GMP rules generated for the graph implementation of LMMSE estimation in [5]–[8] are operated on the constructed graph in which all state variables are assumed to have Gaussian distribution. Therefore, each state variable is represented by a mean and variance value on the graph which makes it a suitable receiver for higher order constellations. Before going into the details of message passing rules, we begin with the state space representation of the system presented in Section II to construct the graph structure. For the system described in Figure 1, the observation vector at time k given in (1) can be rewritten as

$$\mathbf{y}_k = \overline{\mathbf{H}}\, \overline{\mathbf{x}}_k + \mathbf{n}_k \; ; \quad k = 1, 2, \ldots, N + J \tag{7}$$

where

$$\overline{\mathbf{H}} = [\mathbf{H}_J \quad \mathbf{H}_{J-1} \quad \ldots \quad \mathbf{H}_0], \quad \text{and} \tag{8}$$

$$\overline{\mathbf{x}}_k = \begin{bmatrix} \mathbf{x}_{k-J} \\ \mathbf{x}_{k-J+1} \\ \vdots \\ \mathbf{x}_k \end{bmatrix}_{N_t L \times 1} . \tag{9}$$

We use (7)-(9) to construct the state space graph representation of the MIMO ISI channels similar to [17] which discusses the SISO ISI channel case. For transitions to the next time instant, $k + 1$, we define

$$\mathbf{G} = \begin{bmatrix} \mathbf{0}_{N_t J \times N_t} & \mathbf{I}_{N_t J} \\ \mathbf{0}_{N_t \times N_t} & \mathbf{0}_{N_t \times N_t J} \end{bmatrix}_{N_t L \times N_t L} , \tag{10}$$

$$\mathbf{F} = \begin{bmatrix} \mathbf{0}_{N_t J \times N_t} \\ \mathbf{I}_{N_t} \end{bmatrix}_{N_t L \times N_t} \tag{11}$$

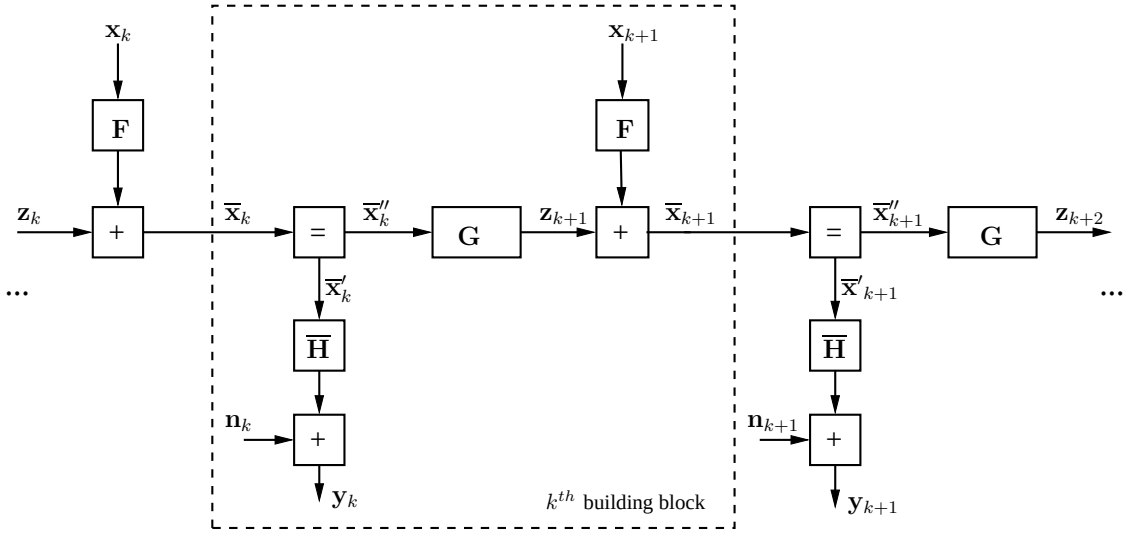

Fig. 2: Factor Graph of MIMO ISI Channel

where $\mathbf{0}$ denotes the all zero matrix of the specified size and $\mathbf{I}_j$ denotes the identity matrix of size j. It can be seen that

$$\overline{\mathbf{x}}_{k+1} = \mathbf{F}\,\mathbf{x}_{k+1} + \mathbf{z}_{k+1}, \quad \text{where} \tag{12}$$

$$\begin{aligned} \mathbf{z}_{k+1} &= \mathbf{G}\,\overline{\mathbf{x}}_k \\ &= \begin{bmatrix} \mathbf{x}_{k-J+1} \\ \mathbf{x}_{k-J+2} \\ \vdots \\ \mathbf{x}_k \\ \mathbf{0}_{N_t \times 1} \end{bmatrix}. \end{aligned} \tag{13}$$

The factor graph representation corresponding to (7)-(13) can be seen in Figure 2. LMMSE equalization is performed on this graph with the help of the GMP rules which are first proposed in [5] and later discussed in [6]–[8], [17]. Each state variable vector on the factor graph is assumed to have Gaussian distribution and represented by a mean vector $(\mathbf{m}_{\overline{\mathbf{x}}_k})$ and a covariance matrix

$(\mathbf{V}_{\overline{\mathbf{x}}_k})$. *A posteriori* mean $(\mathbf{m}_{\overline{\mathbf{x}}_k}^{post})$ and covariance $(\mathbf{V}_{\overline{\mathbf{x}}_k}^{post})$ of the state variables are calculated through the GMP rules which are applied in forward and backward recursions by use of the observations $(\mathbf{y})$ and the *a priori* information $(\mathbf{m}_{\mathbf{x}_k}^{\downarrow},\mathbf{V}_{\mathbf{x}_k}^{\downarrow})$ coming from the APP decoder. In Table I of Appendix B, some of the GMP rules for basic blocks [7], [17] are provided for self-containment. Those rules could be directly applied to the building blocks of the graph in Figure 2.

However, the direct application results in quite a few N_tL-size matrix inversions each of which costs $O(N_t^3L^3)$. Hence, we also list the GMP rules for composite blocks obtained by matrix inversion lemma [25] in Table II of Appendix B to reduce the computational complexity. A brief description of the forward and backward recursion algorithms which use the given GMP rules is provided below for the k^{th} building block. The arrows are used so as to show the direction of the messages as a similar notation to [6]–[8], [17].

- ***Forward Recursion:*** We aim to reach the information related to the state $\overline{\mathbf{x}}_{k+1}$ by use of the known values of the state $\overline{\mathbf{x}}_k$ obtained by the previous building block and the operations given below. Following the direction from left to right on the k^{th} building block of the graph in Figure 2, we compute $\overrightarrow{\mathbf{m}}_{\overline{\mathbf{x}}_k''}$ and $\overrightarrow{\mathbf{V}}_{\overline{\mathbf{x}}_k''}$ by using $\overrightarrow{\mathbf{m}}_{\overline{\mathbf{x}}_k}$, $\overrightarrow{\mathbf{V}}_{\overline{\mathbf{x}}_k}$ coming from the previous building block and the observation vector $\mathbf{y}_k$ through (62)-(63). As the next step for the calculation of $\overrightarrow{\mathbf{m}}_{\mathbf{z}_{k+1}}$ and $\overrightarrow{\mathbf{V}}_{\mathbf{z}_{k+1}}$, we use (58)-(59). With the obtained $\overrightarrow{\mathbf{m}}_{\mathbf{z}_{k+1}}$, $\overrightarrow{\mathbf{V}}_{\mathbf{z}_{k+1}}$ values and the *a priori* information provided by the APP decoder $(\mathbf{m}_{\mathbf{x}_{k+1}}^{\downarrow}, \mathbf{V}_{\mathbf{x}_{k+1}}^{\downarrow})$, the mean and variance values of the state vector $\overline{\mathbf{x}}_{k+1}$ are computed by (54),(56),(58),(59) and used in the next building block as input. By repeating this process for all the building blocks in a serial order, forward recursion is completed.

- ***Backward Recursion:*** In each building block, the purpose is to obtain the weight matrix and the weighted mean vector of the state $\overline{\mathbf{x}}_k$ from the known information related to the state $\overline{\mathbf{x}}_{k+1}$ provided by the previous building block. Following the direction from right to left on the k^{th} building block, first we compute $\overleftarrow{\mathbf{W}}_{\mathbf{z}_{k+1}}$, $\overleftarrow{\mathbf{W}}_{\mathbf{z}_{k+1}}\overleftarrow{\mathbf{m}}_{\mathbf{z}_{k+1}}$ through (65)-(66) with the help of the *a priori* information coming from the APP decoder $(\mathbf{m}_{\mathbf{x}_{k+1}}^{\downarrow},$

$\mathbf{V}^{\downarrow}_{\mathbf{x}_{k+1}}$) and the obtained information of the state $\overline{\mathbf{x}}_{k+1}$ ($\overleftarrow{\mathbf{W}}_{\overline{\mathbf{x}}_{k+1}}$, $\overleftarrow{\mathbf{W}}_{\overline{\mathbf{x}}_{k+1}}\overleftarrow{\mathbf{m}}_{\overline{\mathbf{x}}_{k+1}}$) by the previous building block. Then, after $\overleftarrow{\mathbf{W}}_{\overline{\mathbf{x}}''_k}$ and $\overleftarrow{\mathbf{W}}_{\overline{\mathbf{x}}''_k}\overleftarrow{\mathbf{m}}_{\overline{\mathbf{x}}''_k}$ are computed by (60)-(61), they are utilized in (52)-(53),(60)-(61) together with the observation vector $\mathbf{y}_k$ so as to reach $\overleftarrow{\mathbf{W}}_{\overline{\mathbf{x}}_{k+1}}$, $\overleftarrow{\mathbf{W}}_{\overline{\mathbf{x}}_{k+1}}\overleftarrow{\mathbf{m}}_{\overline{\mathbf{x}}_{k+1}}$. These operations are applied to each building block serially in a similar way to forward recursion except message passing direction.

When forward and backward recursion is completed, the output mean and covariance variance of each state vector $\overline{\mathbf{x}}_k$ are calculated with the help of the obtained ($\overrightarrow{\mathbf{V}}_{\overline{\mathbf{x}}_k}, \overrightarrow{\mathbf{m}}_{\overline{\mathbf{x}}_k}$) and ($\overleftarrow{\mathbf{W}}_{\overline{\mathbf{x}}_k}, \overleftarrow{\mathbf{W}}_{\overline{\mathbf{x}}_k}\overleftarrow{\mathbf{m}}_{\overline{\mathbf{x}}_k}$) as in [5], [17]:

$$\mathbf{V}^{post}_{\overline{\mathbf{x}}_k} = (\overrightarrow{\mathbf{V}}^{-1}_{\overline{\mathbf{x}}_k} + \overleftarrow{\mathbf{W}}_{\overline{\mathbf{x}}_k})^{-1} \tag{14}$$

$$\mathbf{m}^{post}_{\overline{\mathbf{x}}_k} = \mathbf{V}^{post}_{\overline{\mathbf{x}}_k}(\overrightarrow{\mathbf{V}}^{-1}_{\overline{\mathbf{x}}_k}\overrightarrow{\mathbf{m}}_{\overline{\mathbf{x}}_k} + \overleftarrow{\mathbf{W}}_{\overline{\mathbf{x}}_k}\overleftarrow{\mathbf{m}}_{\overline{\mathbf{x}}_k})^{-1} \tag{15}$$

The diagonal elements of $\mathbf{V}^{post}_{\overline{\mathbf{x}}_k}$ give the *a posteriori* variance values of the symbols sent from all transmit antennas between the time instants $k-J$ and k as given by

$$\mathbf{V}^{post}_{\overline{\mathbf{x}}_k} = \begin{bmatrix} \mathbf{V}^{post}_{\mathbf{x}_{k-J}} & \cdots & \cdots \\ \cdots & \mathbf{V}^{post}_{\mathbf{x}_{k-J+1}} & \cdots \\ \cdots & \ddots & \cdots \\ \cdots & \cdots & \mathbf{V}^{post}_{\mathbf{x}_k} \end{bmatrix}, \quad \text{where} \tag{16}$$

$$diag\{\mathbf{V}^{post}_{\overline{\mathbf{x}}_k}\} = [diag\{\mathbf{V}^{post}_{\mathbf{x}_{k-J}}\} \quad diag\{\mathbf{V}^{post}_{\mathbf{x}_{k-J+1}}\} \ldots \tag{17}$$

$$\ldots diag\{\mathbf{V}^{post}_{\mathbf{x}_k}\}], \quad \text{and}$$

$$diag\{\mathbf{V}^{post}_{\mathbf{x}_k}\} = [v^{post}_{x_{k,1}} \; v^{post}_{x_{k,2}} \; \ldots \; v^{post}_{x_{k,N_t}}]. \tag{18}$$

In a similar way, the elements of $\mathbf{m}^{post}_{\overline{\mathbf{x}}_k}$ includes the *a posteriori* mean values of the state vector

$\overline{\mathbf{x}}_k$ as below:

$$\mathbf{m}^{post}_{\overline{\mathbf{x}}_k} = \begin{bmatrix} \mathbf{m}^{post}_{\mathbf{x}_{k-J}} \\ \mathbf{m}^{post}_{\mathbf{x}_{k-J+1}} \\ \vdots \\ \mathbf{m}^{post}_{\mathbf{x}_k} \end{bmatrix}, \text{ where } \quad \mathbf{m}^{post}_{\mathbf{x}_k} = \begin{bmatrix} m^{post}_{x_{k,1}} \\ m^{post}_{x_{k,2}} \\ \vdots \\ m^{post}_{x_{k,N_t}} \end{bmatrix}. \tag{19}$$

Since the elements of the state vector $\overline{\mathbf{x}}_k$ is shifted by N_t symbols through the way to $\overline{\mathbf{x}}_{k+1}$, this shift is also seen at the output mean vectors and variance matrices as below:

$$\mathbf{V}^{post}_{\overline{\mathbf{x}}_{k+1}} = \begin{bmatrix} \mathbf{V}^{post}_{\mathbf{x}_{k-J+1}} & \dots & \dots \\ \dots & \mathbf{V}^{post}_{\mathbf{x}_{k-J+2}} & \dots \\ \dots & \ddots & \dots \\ \dots & \dots & \mathbf{V}^{post}_{\mathbf{x}_{k+1}} \end{bmatrix}, \; \mathbf{m}^{post}_{\overline{\mathbf{x}}_{k+1}} = \begin{bmatrix} \mathbf{m}^{post}_{\mathbf{x}_{k-J+1}} \\ \mathbf{m}^{post}_{\mathbf{x}_{k-J+2}} \\ \vdots \\ \mathbf{m}^{post}_{\mathbf{x}_{k+1}} \end{bmatrix}. \tag{20}$$

It should be noted that the symbols sent from different transmit antennas are assumed to be independent. So, the *a priori* information related to $\mathbf{x}_k$ is involved in the factor graph as

$$\mathbf{m}^{\downarrow}_{\mathbf{x}_k} \triangleq \mathbf{m}^{prio}_{\mathbf{x}_k} = \begin{bmatrix} m^{prio}_{x_{k,1}} & m^{prio}_{x_{k,2}} & \dots & m^{prio}_{x_{k,N_t}} \end{bmatrix}^T, \tag{21}$$

$$\mathbf{V}^{\downarrow}_{\mathbf{x}_k} \triangleq \mathbf{V}^{prio}_{\mathbf{x}_k} = \begin{bmatrix} v^{prio}_{x_{k,1}} & 0 & \dots & 0 \\ 0 & v^{prio}_{x_{k,2}} & \ddots & \vdots \\ \vdots & \ddots & \ddots & 0 \\ 0 & \dots & 0 & v^{prio}_{x_{k,N_t}} \end{bmatrix} \tag{22}$$

where $m^{prio}_{x_{k,l}}$ and $v^{prio}_{x_{k,l}}$ are the mean and variance values computed under the Gaussian assumption by using the LLR values obtained by APP decoder.

An algorithm is needed to convert the output of the LMMSE equalizer, which is in the form of mean and variance values at this point, to the extrinsic bit LLRs. In the next section, we propose an algorithm consistent with the factor graph to maintain the low complexity for higher order alphabets.

IV. LLR EXCHANGE ALGORITHM COMPATIBLE WITH THE GRAPH APPROACH

LMMSE equalizer used in turbo decoders needs an algorithm to transit between binary, i.e., bit LLR domain, and Gaussian domain. There are mathematical models for the extrinsic bit LLR computation of the LMMSE equalizer in the literature such as the WP [19], [20] and the JG approaches [21] which are not suitable for the graph based LMMSE equalization due to their high computational complexity caused by matrix inversions of size $N_t N$. In [17], considering the graph outputs, the mathematical expression of the extrinsic bit LLRs with respect to the JG approach was simplified for BPSK signaling. Also, the authors of [17] shows the equivalence between the JG and WP approaches for BPSK signaling. However, there is no mathematically justified reduced complexity LLR exchange algorithm for higher constellation sizes in the literature to the best of our knowledge. Despite the fact [22] proposed an intuitive method for M-QAM signaling without any simulation results, we have observed that equation (8) in [22] causes both diversity and SNR losses as shown in Section IV-A. Moreover, we have also proposed a heuristic algorithm in which both the intrinsic and the a priori LLRs are computed under the Gaussian assumption presented in [23]. Although it has much better performance than the one in [22] for M-QAM signaling, there exists no scientifically proved basis for the idea behind our heuristic method. Also, as given in the comparative results in Section IV-A, the WP approach simplified here, on which we will base our proposal, is observed to perform better for M-QAM signaling in comparison to both methods in [22], [23].

In the subsequent section, we provide the mathematical relation between the graph based LMMSE equalizer outputs (*a posteriori* mean and variance values) and the bit LLRs for higher order modulation alphabets. Hence, owing to this key connection, extrinsic bit LLR values from

LMMSE estimation can be obtained easily in accordance with the graph solution without any major complexity increase.

A. Simplified WP Approach for Graph Based LMMSE Estimation

WP approach is a famous extrinsic bit LLR computation method for LMMSE estimation which was first presented in [19] and later proposed to be used in iterative decoder structures in [20] for SISO systems. Since the input symbols are independent and identically distributed, the multiple number of transmit and receive antennas results in just an enlargement in signalling space and does not pose a problem to utilize WP approach for our MIMO system.

For clear understanding, we can rewrite the system model presented in (4) as

$$\mathbf{y} = \sum_{k=1}^{N} \sum_{j=1}^{N_t} \mathbf{h}_{k,j}\, x_{k,j} + \mathbf{n} \tag{23}$$

where $\mathbf{h}_{k,j}$ is the $((k-1)N_t + j)^{th}$ column vector of the channel convolution matrix $\mathbf{H}$ which corresponds to $x_{k,j}$ as given by

$$\mathbf{H} = [\mathbf{h}_{1,1} \ldots \mathbf{h}_{1,N_t} \ldots\ldots \mathbf{h}_{k,1} \ldots \mathbf{h}_{k,j} \ldots \mathbf{h}_{k,N_t} \ldots \mathbf{h}_{N,N_t}] \tag{24}$$

According to the WP approach, Gaussian approximation is held after the LMMSE equalization process [19], [20]. In other words, the residual interference plus noise term at the output of the LMMSE equalizer can be well approximated by Gaussian distribution [19], [20]. Hence, the filtered observation at time k for the j^{th} transmit antenna $(\hat{x}_{k,j})$ given an input symbol is assumed to have Gaussian distribution, i.e., the probability density function (pdf) of $p(\hat{x}_{k,j}|x_{k,j} = s) \sim N(\mu_{k,j}s, \sigma_{k,j})$ with $s \in S$ where S is the modulation alphabet [20]. An equivalent model for this approximation can be written similarly to [19] as

$$\hat{x}_{k,j} = \mu_{k,j}\, x_{k,j} + \eta_{k,j}, \quad k = 1, \ldots, N \;\; j = 1, \ldots, N_t \tag{25}$$

where $\eta_{k,j} \sim N(0, \sigma_{k,j})$. To reach the extrinsic information following the same method in [20], we rearrange the expression of the filtered observation at time k for the j^{th} transmit antenna by

setting $m_{x_{k,j}}^{prio} = 0$ and $v_{x_{k,j}}^{prio} = 1$ so that it does not depend on the current *a priori* information $(m_{x_{k,j}}^{prio}, v_{x_{k,j}}^{prio})$, which gives

$$\hat{x}_{k,j} = \mathbf{w}_{k,j}^H(\mathbf{y} - \mathbf{H}\mathbf{m}_{\mathbf{x}}^{prio} + m_{x_{k,j}}^{prio}\,\mathbf{h}_{k,j}) \tag{26}$$

where $\mathbf{w}_{k,j}$ is the LMMSE filter coefficient vector with length $N_r(N+J)$ for the k^{th} transmitted input symbol from the j^{th} antenna as expressed by

$$\mathbf{w}_{k,j} = (N_0\mathbf{I}_{N_r(N+J)} + \sum_{\substack{i=1 \\ i\neq k}}^{N} v_{x_{i,j}}^{prio}\mathbf{h}_{i,j}\mathbf{h}_{i,j}^H + \mathbf{h}_{k,j}\mathbf{h}_{k,j}^H)^{-1}\mathbf{h}_{k,j} \tag{27}$$

and, $\mu_{k,j}$ and $\sigma_{k,j}$ are obtained as [20]

$$\mu_{k,j} = \mathbf{w}_{k,j}^H\,\mathbf{h}_{k,j} \tag{28}$$

$$\sigma_{k,j}^2 = \mathbf{w}_{k,j}^H\,\mathbf{h}_{k,j}(1 - \mathbf{h}_{k,j}^H\,\mathbf{w}_{k,j}) \tag{29}$$

$$= \mu_{k,j}(1 - \mu_{k,j}^H). \tag{30}$$

If the k^{th} transmitted symbol from the j^{th} antenna is represented by b bits of $[c_{k,j}^1\ c_{k,j}^2\ \ldots\ c_{k,j}^b]$, then the extrinsic LLR value of the q^{th} bit of the k^{th} symbol from the j^{th} antenna could be expressed by considering the Gaussian assumption in (25) as

$$L_E(c_{k,j}^q) = \ln\left(\frac{\sum_{s\in S_{q,0}} p(x_{k,j}=s|\hat{x}_{k,j})}{\sum_{s\in S_{q,1}} p(x_{k,j}=s|\hat{x}_{k,j})}\right) - \ln\left(\frac{\sum_{s\in S_{q,0}} p(x_{k,j}=s)}{\sum_{s\in S_{q,1}} p(x_{k,j}=s)}\right)$$
$$q = 1, 2, \ldots, b \tag{31}$$

where $S_{q,0}$ $(S_{q,1})$ denotes the subset of the modulation alphabet S with symbols whose q^{th} bit is 0 (1), and $p(x_{k,j}=s)$'s are the *a priori* symbol probability for the k^{th} transmitted symbol from the j^{th} antenna. Using Bayes Rule [26], (31) can be rewritten by considering the Gaussian

assumption in (25) as

$$L_E(c_{k,j}^q) = \ln\left(\frac{\sum_{s\in S_{q,0}} p(\hat{x}_{k,j}|x_{k,j}=s)p(x_{k,j}=s)}{\sum_{s\in S_{q,1}} p(\hat{x}_{k,j}|x_{k,j}=s)p(x_{k,j}=s)}\right) - \ln\left(\frac{\sum_{s\in S_{q,0}} p(x_{k,j}=s)}{\sum_{s\in S_{q,1}} p(x_{k,j}=s)}\right) \quad q=1,2,\ldots,b \tag{32}$$

where

$$p(\hat{x}_{k,j}|x_{k,j}=s) \propto \exp(-|\hat{x}_{k,j}-\mu_{k,j}s|^2/\sigma_{k,j}^2). \tag{33}$$

As can be seen in (26-30), the complexity of finding $\hat{x}_{k,j}$, $\mu_{k,j}$ and $\sigma_{k,j}$ values is $O(N^3N_r^3)$ and mainly determined by (27) which involves a matrix inversion of size $N_r(N+J)$. Moreover, there is no mathematical simplification in the extrinsic bit LLR expression in (32) for M-QAM signalling due to the summation over symbols unlike the BPSK signalling case discussed in [17]. Hence, this version of WP approach is not suitable for the graph based LMMSE equalization. The expressions in Proposition 1 below provide the key connection between the graph outputs (*a posteriori* mean and variance values) and the WP parameters ($\hat{x}_{k,j}$, $\mu_{k,j}$ and $\sigma_{k,j}$) with no major complexity increase.

Proposition 1: WP parameters necessary to evaluate the extrinsic LLR can be found based on the graph outputs, namely a posteriori mean and variance values, through expressions

$$\hat{x}_{k,j} = \left(\frac{m_{x_{k,j}}^{post}}{v_{x_{k,j}}^{post}} - \frac{m_{x_{k,j}}^{prio}}{v_{x_{k,j}}^{prio}}\right) \Big/ \left(1 + \frac{1}{v_{x_{k,j}}^{post}} - \frac{1}{v_{x_{k,j}}^{prio}}\right), \tag{34}$$

$$\frac{\mu_{k,j}}{\sigma_{k,j}^2} = \left(1 + \frac{1}{v_{x_{k,j}}^{post}} - \frac{1}{v_{x_{k,j}}^{prio}}\right). \tag{35}$$

The proof of Proposition 1 is given in Appendix A.

With the help of (30) and (34-35), the parameters of WP method ($\hat{x}_{k,j}$, $\mu_{k,j}$, $\sigma_{k,j}$) are easily computed by applying simple operations to the graph outputs and utilized in (32) to reach the extrinsic bit LLRs related to each transmitted symbol. When we consider the computational complexity of the proposed extrinsic bit LLR computation algorithm, the dominant contribution

is due to (32) which has $O(NN_tM\log_2 M)$ complexity per turbo iteration. To reach the overall complexity of the presented turbo receiver structure, one may consider this part, too. However, any equalizer structure using M-QAM modulation requires an algorithm to obtain the bit LLR values from the symbol probabilities which results in a complexity similar to that of (32).

For a SISO system, the method described above can be easily adapted by setting $N_t = N_r = 1$ that removes the index j in (23)-(35) which indicates the transmit antenna number.

B. Simulation Results for the Simplified WP Approach

The performance results of our proposed extrinsic bit LLR computation method for 64-QAM signalling as compared to the ones in [22], [23] are given in Figure 3. Simulations are conducted for a SISO system under the static ISI channel whose tap amplitudes are given by $\overline{\mathbf{h}} = \frac{1}{\sqrt{6}}[1\ 2\ 0\ 0\ 0\ 1]$. A convolutional code with rate $1/2$ and generator polynomial $(133, 171)$ is used, and the LMMSE equalizer is operated in a turbo decoder using 5 iterations.

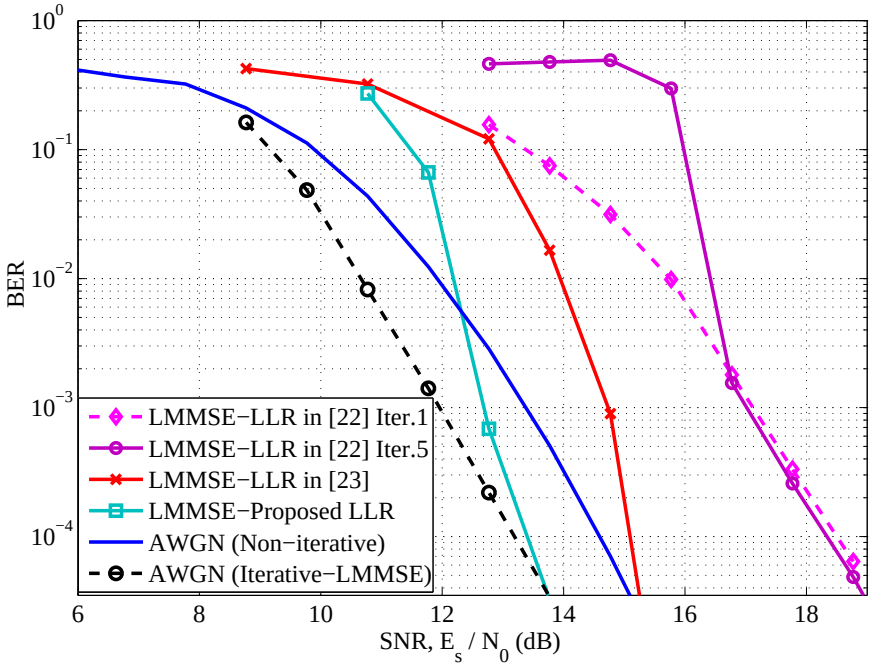

Fig. 3: Performance Comparison of Extrinsic LLR Computation Algorithms for LMMSE Equalizer (64-QAM with ISI Channel of $\frac{1}{\sqrt{6}}[1\ 2\ 0\ 0\ 0\ 1]$)

To serve as a benchmark for the performances in ISI channel, we also simulate the LMMSE equalizer under 3 turbo iterations for AWGN (single-tap) channel shown by black dashed line called AWGN (Iterative-LMMSE). In addition, the blue solid line, called AWGN (Non-iterative), shows the non-iterative receiver performance for AWGN channel. To obtain this performance, the APP decoder is operated only once by using the bit LLR values which are generated from the conditional probabilities given each of 64 points in the constellation for each input symbol. The explicit computation of the LLR value of the q^{th} bit of k^{th} symbol entered to the APP decoder, $L_{AWGN,NI}$, is

$$L_{AWGN,NI}(c_k^q) = \ln\left(\frac{\sum_{s\in S_{q,0}} p(y_k|x_k=s)}{\sum_{s\in S_{q,1}} p(y_k|x_k=s)}\right) \quad q=1,2,\ldots,b \tag{36}$$

where

$$p(y_k|x_k=s) \propto \exp(-|y_k-s|^2/N_0), \tag{37}$$

and $S_{q,0}$ $(S_{q,1})$ denotes the subset of the modulation alphabet S with symbols whose q^{th} bit is 0 (1). It should be noted that in Figure 3, performance difference is observed between the iterative and the non-iterative receivers under AWGN channel. The reason is that the BER performance is improved by turbo iterations under the bit interleaved coded modulation with such a large signalling space (64-QAM) even in AWGN channel as studied in [27], [28].

Among the LMMSE equalizer performances, it is seen that at 10^{-4} BER level, there is more than 4 dB and nearly 2 dB gain of the proposed method with respect to the LLR exchange schemes in [22] and [23] respectively. Another important point to mention is that the method in [22] given by equation (8) leads to no improvement in performance as the number of turbo iterations increases. Also, our previous heuristic method described in [23] needs a scaling operation which multiplies the bit LLR values at the output of the LMMSE equalizer to reach the presented performance in Figure 3. Since finding the optimal scalar value requires exhaustive search for each different configuration, the method in [23] is not a practical solution either. Hence, the simplified version of the Wang Poor approach for factor graphs seems to be the

best choice for M-QAM modulation among the other proposed solutions. Therefore, we use this method for the LLR computation in the rest of our study.

C. Convergence Properties of the Proposed Receiver

In this section, the convergence properties of the proposed LLR exchange algorithm for the LMMSE equalizer are investigated. For this purpose, we observe the evolution of the mutual information between the transmitted bit and the corresponding LLR value similar to the studies in [29]–[31]. More specifically, *the information content function* for the MIMO system in (7) is written as given in [29], [30]

$$I(Z) = \frac{1}{NN_t b} \sum_{k=1}^{N} \sum_{j=1}^{N_t} \sum_{q=1}^{b} \left[1 - \log_2(1 + \exp(-Z_{k,j}^q))\right], \tag{38}$$

where $Z = \{Z_{k,j}^q\}$ is the extrinsic information sequence in log domain for all the bits sent over the transmit antennas and its elements are expressed as

$$Z_{k,j}^q = (-1)^{c_{k,j}^q} L(c_{k,j}^q), \tag{39}$$

and $L(c_{k,j}^q)$ in (39) denotes the extrinsic bit LLR value related to the q^{th} bit of the k^{th} transmitted symbol from the j^{th} antenna.

Since we are interested in the reliability at the output of the APP decoder after each turbo iteration, we compute (38) by taking $L(c_{k,j}^q) = L_{APP}(c_{k,j}^q)$ in (39) where $L_{APP}(c_{k,j}^q)$ denotes the extrinsic bit LLR values at the output of the APP decoder. Using Monte Carlo simulations for the SISO-ISI scenario under 64-QAM detailed in Section IV-B, we obtain the average information content at the output of the APP decoder with respect to the number of turbo iterations for different SNR values. Consequently, the resulting convergence characteristics of the proposed LLR exchange method is given in Figure 4.

It can be seen in Figure 4 that the reliability of the extrinsic information converges to a point with the growing number of turbo iterations. Moreover, for larger SNR values, the information content converges to a larger value (meaning more reliable estimation) much faster. For example,

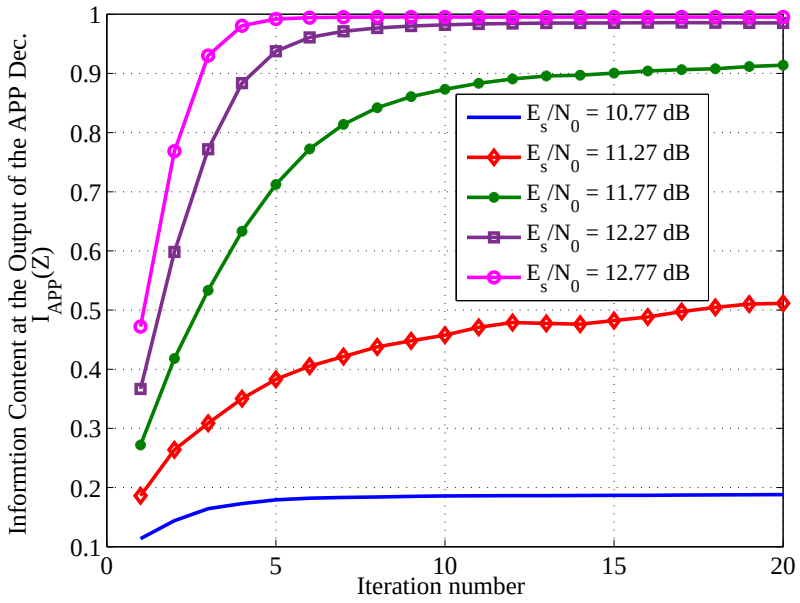

Fig. 4: Convergence Characteristics of the Proposed LLR Exchange Algorithm (64-QAM with ISI Channel of $\frac{1}{\sqrt{6}}[1\ 2\ 0\ 0\ 0\ 1]$)

for $E_s/N_0 = 12.77$ dB, only 5 turbo iterations are sufficient for the information content to converge to a much higher value than the convergence points for smaller SNR values.

Overall, LMMSE equalization with the proposed extrinsic LLR exchange method is advantageous with its reduced complexity, superior performance results and satisfactory convergence properties.

V. COMPLEXITY ANALYSIS

The major contribution to the complexity of the proposed graph structure is caused by the matrix inversions in (14-15), (64) and (67). In each building block, (64) and (67) need to be calculated with a complexity of $O(N_r^3)$ since they involve matrix inversions of size N_r thanks to the applied matrix inversion lemma. On the other hand, (14) and (15) are applied only once for every L building blocks with a complexity of $O(N_t^3 L^3)$ owing to the shifting property of the state vectors as observed in (20). Hence, it corresponds to $O(N_t^3 L^2)$ for each building block, i.e., each time instant, where there are N building blocks in our system. Therefore, the overall complexity

is $O(N \cdot max\{N_r^3, N_t^3 L^2\})$ which is equal to $O(NN_t^3 L^2)$ in most of the cases. As a result of this discussion, the overall complexity per symbol per transmit antenna is $O(N_t^2 L^2)$. To reach the bit level complexity, we need to add $O(NN_t M \log_2 M)$ complexity of bit LLR computation method described in Section IV. However, to make a fair comparison to the previous studies, we continue with the complexity for symbol level, i.e., $O(NN_t^3 L^2)$ since they gave their complexity analysis in this form.

When we consider other methods in the literature, [12] proposed the belief propagation over factor graphs for frequency selective MIMO systems with a complexity of $O(NM^{N_t \tilde{L}})$ where $\tilde{L}$ is the number of non-zero channel taps. When a high order modulation alphabet is used in a dense channel, $O(NM^{N_t \tilde{L}})$ is much greater than $O(NN_t^3 L^2)$ complexity of our method. In addition, the proposed Kalman filtering solution in [13], which is deprived from the improvement of backward recursion (Kalman smoothing), has a complexity of $O(NN_t^3 L^3)$. Also, the complexity of the lately studied LMMSE equalizer in [18] which was proposed to implement using a different factor graph structure from ours is $O(NN_t^3 L^3)$ which is still greater than the complexity of the structure in this study. Moreover, although the result of the LMMSE estimation in [18] is the same as our graph output on Gaussian domain, it results in an error floor for large SNR values due to their LLR exchange algorithm between Gaussian and binary domains. Overall, our proposed LMMSE solution is a practical receiver for high data rate applications with its lower complexity than those presented in the literature and its close performance to matched filter bound to be presented in the subsequent section.

VI. SIMULATION RESULTS

We conduct our simulations under quasi-static Rayleigh fading channels with independent ISI taps, i.e., each tap is constant over one block and change independently from block to block. The ISI channel between each transmit-receive antenna pair has identical, equal power delay profile, i.e., all L taps have equal power which is normalized so that the total power of channel

response is unity,

$$\sum_{k=0}^{L-1} E\{|h_{ij}(k)|^2\} = 1, \tag{40}$$

where $h_{ij}(k)$ is the k^{th} channel tap between the j^{th} transmit antenna and i^{th} receive antenna. The simulations are based on the system model in Figure 1 with a random interleaver and a rate $1/2$ convolution code whose generator matrix is $(7, 5)_8$ under the modulation types of BPSK and 16-QAM. In all simulations, there are a total of 4096 data bits which are coded, interleaved and then modulated. The modulated symbols are distributed to the transmit antennas by a spatial multiplexing operation as given in Figure 1.

For the LLR exchange process between the LMMSE equalizer and the APP decoder, we use the WP approach explained in Section IV. With our proposed bit LLR exchange algorithm, there is no need to apply scaling operations to the extrinsic LLR values at the output of the LMMSE equalizer and the APP decoder to improve the performance contrary to the turbo decoding algorithms in the literature [15], [16], [32], [33].

For all the configurations below, we also provide the matched filter bound (MFB) performances as a benchmark to make a comparison. The MFB performances are obtained under the assumption that the symbols which cause interference to the interested symbol due to multi-path and multi-antenna effects are perfectly known by the receiver for each interested symbol [24]. Hence, it is practically impossible to reach MFB performance for any receiver structure. We take MFB performance as a genie-aided lower bound for the proposed scheme.

The bit error ratio (BER) performance of the proposed factor graph based LMMSE equalizer is given in Figure 5 for BPSK signalling with $N_t = N_r = 2$ under a 5-tap channel. This is the same configuration as the one in [18] except the interleaver type which is S-random in [18]. The proposed method has nearly identical performance with the one in [18] for low SNR values as expected since both algorithms implement time domain LMMSE filtering operation. Moreover, the error floor observed in high SNR regions in [18], which is caused by its extrinsic LLR exchange algorithm, does not occur here. Also, the performance of the proposed method is very

close to the MFB below the BER value of 10^{-3} without any diversity loss or error floor. In addition, it can be seen that there is no significant improvement after 3 turbo iterations which means only 3 iterations are sufficient for this configuration.

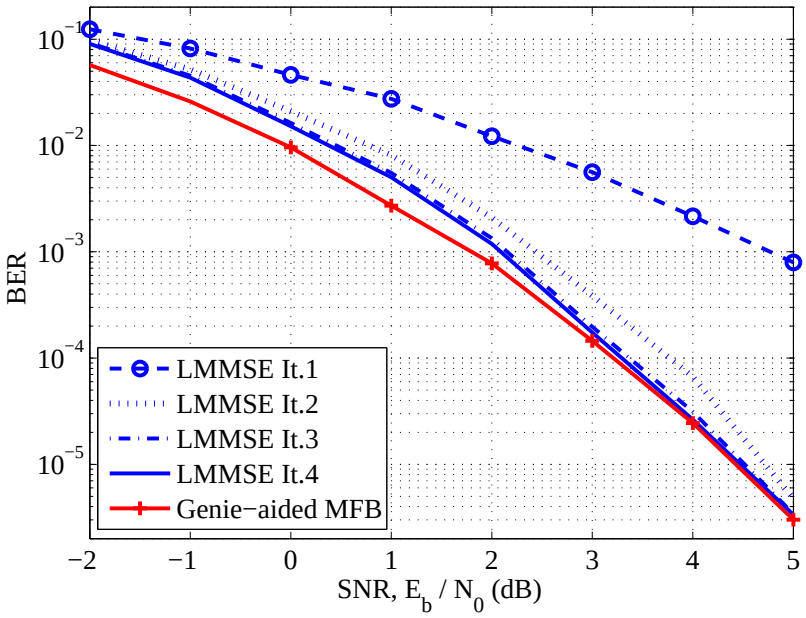

Fig. 5: BER Performance of the Factor Graph Based LMMSE Equalizer (2×2 MIMO with $L = 5$ for BPSK Signaling)

Also, we would like to present the performance of a more challenging scenario with higher order constellations which was not presented in the studies including Gaussian approximation over a factor graph in the literature so far. Figure 6 depicts simulation results for 16-QAM signaling under a 4-tap ISI channel with $N_t = N_r = 2$. It can be seen from Figure 6 that the proposed method has a performance which is less than 1 dB away from the MFB performance below the BER value of 10^{-4} for 7 turbo iterations. The increased constellation size leads to a higher number of turbo iterations for good performance, but turbo iteration number is not a direct multiplier of computational complexity since all packets do not require 7 iterations. Moreover, the constellation size M is included only in the complexity term related to the bit LLR computation method in a linearly increasing fashion. Hence, our method is a practical

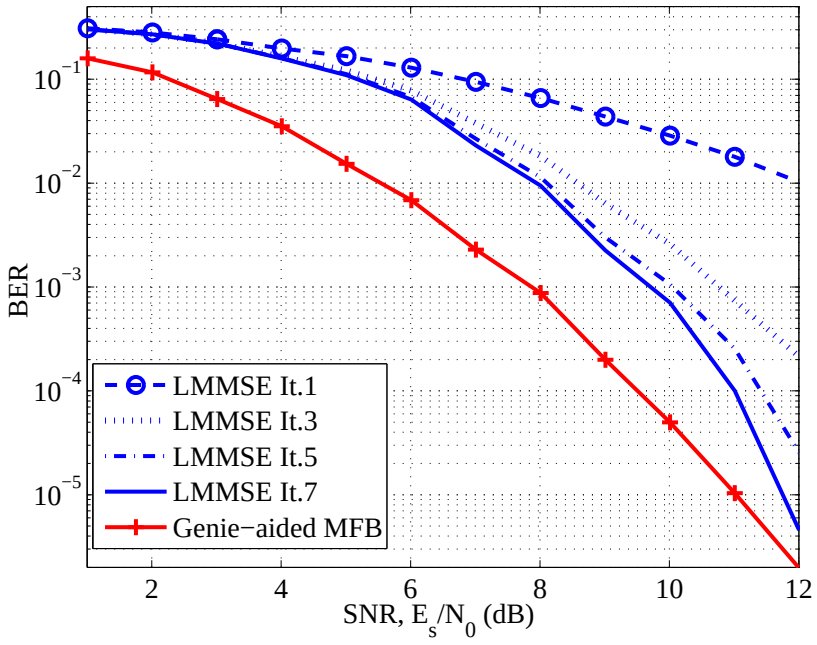

Fig. 6: BER Performance of the Factor Graph Based LMMSE Equalizer (2×2 MIMO with $L = 4$ for 16-QAM Signaling)

choice as a receiver structure with its solid performance while achieving higher data rates.

VII. CONCLUSION

In this study, we developed a factor graph structure for the LMMSE equalization of frequency selective MIMO channels. Our proposed graph has the advantage of low complexity as compared to the conventional block LMMSE filtering operation and the other graph based LMMSE filtering approaches in the literature. In addition, we provided an efficient way of computing extrinsic LLR values of LMMSE equalization for M-QAM constellations based on the well-known Wang-Poor (WP) approach with no major complexity increase. In other words, we have shown the mathematical relation between the output of the LMMSE equalizer and the WP parameters in a suitable fashion for factor graph. To sum up, we proposed a low complexity, practical LMMSE equalizer for turbo decoding of MIMO ISI channels with a good performance as confirmed by our simulation results. Our method comes forefront particularly for higher constellation sizes

with its low computational complexity owing to the Gaussian assumption used in the factor graph and the proposed bit LLR exchange algorithm.

VIII. APPENDIX A: PROOF OF PROPOSITION 1

The LMMSE filter coefficient vector for the k^{th} transmitted symbol from the j^{th} transmit antenna, $\mathbf{w}_{k,j}$, previously given in (27) can be rewritten as

$$\mathbf{w}_{k,j} = \left(\mathbf{V}_{\xi_{k,j}} + \mathbf{h}_{k,j}\mathbf{h}_{k,j}^H\right)^{-1}\mathbf{h}_{k,j}, \quad \text{where} \tag{41}$$

$$\mathbf{V}_{\xi_{k,j}} \triangleq N_0\mathbf{I}_{N_r(N+J)} + \sum_{\substack{i=1\\ i\neq k}}^{N} v_{x_{i,j}}^{prio}\mathbf{h}_{i,j}\mathbf{h}_{i,j}^H. \tag{42}$$

By matrix inversion lemma [25], (41) could be simplified to

$$\mathbf{w}_{k,j} = \frac{\mathbf{V}_{\xi_{k,j}}^{-1}\mathbf{h}_{k,j}}{1+\mathbf{h}_{k,j}^H\mathbf{V}_{\xi_{k,j}}^{-1}\mathbf{h}_{k,j}}. \tag{43}$$

Inserting (43) into (26) gives

$$\hat{x}_{k,j} = \frac{\mathbf{h}_{k,j}^H\mathbf{V}_{\xi_{k,j}}^{-1}}{1+\mathbf{h}_{k,j}^H\mathbf{V}_{\xi_{k,j}}^{-1}\mathbf{h}_{k,j}}\left(\mathbf{y} - \mathbf{H}\mathbf{m}_{\mathbf{x}}^{prio} + \mathbf{h}_{k,j}m_{x_{k,j}}^{prio}\right). \tag{44}$$

The outputs of the LMMSE equalizer, the *a posteriori* mean and variance values, are defined in [34] and used in [17] as

$$v_{x_{k,j}}^{post} = \frac{1}{1/v_{x_{k,j}}^{prio} + \mathbf{h}_{k,j}^H\mathbf{V}_{\xi_{k,j}}^{-1}\mathbf{h}_{k,j}} \tag{45}$$

$$m_{x_{k,j}}^{post} = \frac{m_{x_{k,j}}^{prio}/v_{x_{k,j}}^{prio} + \mathbf{h}_{k,j}^H\mathbf{V}_{\xi_{k,j}}^{-1}\left(\mathbf{y} - \mathbf{H}\mathbf{m}_{\mathbf{x}}^{prio} + \mathbf{h}_{k,j}m_{x_{k,j}}^{prio}\right)}{1/v_{x_{k,j}}^{prio} + \mathbf{h}_{k,j}^H\mathbf{V}_{\xi_{k,j}}^{-1}\mathbf{h}_{k,j}}. \tag{46}$$

Using (44)-(46) we obtain

$$\begin{aligned}\left(\frac{m_{x_{k,j}}^{post}}{v_{x_{k,j}}^{post}} - \frac{m_{x_{k,j}}^{prio}}{v_{x_{k,j}}^{prio}}\right) =& \mathbf{h}_{k,j}^H\mathbf{V}_{\xi_{k,j}}^{-1}\left(\mathbf{y} - \mathbf{H}\mathbf{m}_{\mathbf{x}}^{prio} + \mathbf{h}_{k,j}m_{x_{k,j}}^{prio}\right)\\ =& \hat{x}_{k,j}\left(1+\mathbf{h}_{k,j}^H\mathbf{V}_{\xi_{k,j}}^{-1}\mathbf{h}_{k,j}\right).\end{aligned} \tag{47}$$

Combining (45) and (47) provides the expression for $\hat{x}_{k,j}$ in (34) as seen by

$$\hat{x}_{k,j} = \left(\frac{m_{x_{k,j}}^{post}}{v_{x_{k,j}}^{post}} - \frac{m_{x_{k,j}}^{prio}}{v_{x_{k,j}}^{prio}} \right) / \left(1 + \mathbf{h}_{k,j}^{H} \mathbf{V}_{\xi_{k,j}}^{-1} \mathbf{h}_{k,j} \right) \tag{48}$$
$$= \left(\frac{m_{x_{k,j}}^{post}}{v_{x_{k,j}}^{post}} - \frac{m_{x_{k,j}}^{prio}}{v_{x_{k,j}}^{prio}} \right) / \left(1 + \frac{1}{v_{x_{k,j}}^{post}} - \frac{1}{v_{x_{k,j}}^{prio}} \right).$$

In order to derive the expression given in (35), we use (28) and (29) so that the relation between $\sigma_{k,j}$ and $\mu_{k,j}$ is obtained as

$$\frac{\sigma_{k,j}^2}{\mu_{k,j}} = 1 - \mathbf{h}_{k,j}^{H} \mathbf{w}_{k,j}. \tag{49}$$

Inserting the expression for $\mathbf{w}_{k,j}$ in (43) to (49) results in

$$\frac{\mu_{k,j}}{\sigma_{k,j}^2} = 1 + \mathbf{h}_{k,j}^{H} \mathbf{V}_{\xi_{k,j}}^{-1} \mathbf{h}_{k,j}. \tag{50}$$

Using (45) and (50), one reaches

$$1 + \mathbf{h}_{k,j}^{H} \mathbf{V}_{\xi_{k,j}}^{-1} \mathbf{h}_{k,j} = 1 + \frac{1}{v_{x_{k,j}}^{post}} - \frac{1}{v_{x_{k,j}}^{prio}}. \tag{51}$$

The derivations given above provide a mathematical transition between the LMMSE equalizer outputs and the commonly used WP approach for the extrinsic LLR calculation which is very useful particularly for the graph based LMMSE algorithms for M-QAM modulation.

IX. APPENDIX B: GMP RULES FOR BASIC AND COMPOSITE BLOCKS

The GMP rules for basic blocks derived in [7] and later used in [17] are given in Table I. Due to high computational complexity caused by matrix inversion operations in Table I, we present the simplified versions in Table II by using matrix inversion lemma [25] for the composite blocks involved in our factor graph structure in Figure 2.

REFERENCES

[1] G. Guvensen and A. Yilmaz, “A general framework for optimum iterative blockwise equalization of single carrier MIMO systems and asymptotic performance analysis,” *Communications, IEEE Transactions on*, vol. 61, no. 2, pp. 609–619, February 2013.

TABLE I: GMP Rules for Basic Building Blocks [7], [17]

Blocks	GMP Rules	
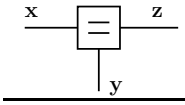	$\overrightarrow{\mathbf{W}}_{\mathbf{z}} = \overrightarrow{\mathbf{W}}_{\mathbf{x}} + \mathbf{W}_{\mathbf{y}}^{\uparrow}$ $\overrightarrow{\mathbf{W}}_{\mathbf{z}}\overrightarrow{\mathbf{m}}_{\mathbf{z}} = \overrightarrow{\mathbf{W}}_{\mathbf{x}}\overrightarrow{\mathbf{m}}_{\mathbf{x}} + \mathbf{W}_{\mathbf{y}}^{\uparrow}\mathbf{m}_{\mathbf{y}}^{\uparrow}$	(52) (53)
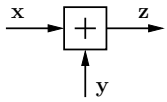	$\overrightarrow{\mathbf{V}}_{\mathbf{z}} = \overrightarrow{\mathbf{V}}_{\mathbf{x}} + \mathbf{V}_{\mathbf{y}}^{\uparrow}$ $\overleftarrow{\mathbf{V}}_{\mathbf{x}} = \overleftarrow{\mathbf{V}}_{\mathbf{z}} + \mathbf{V}_{\mathbf{y}}^{\uparrow}$ $\overrightarrow{\mathbf{m}}_{\mathbf{z}} = \overrightarrow{\mathbf{m}}_{\mathbf{x}} + \mathbf{m}_{\mathbf{y}}^{\uparrow}$ $\overleftarrow{\mathbf{m}}_{\mathbf{x}} = \overleftarrow{\mathbf{m}}_{\mathbf{z}} - \mathbf{m}_{\mathbf{y}}^{\uparrow}$	(54) (55) (56) (57)
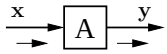	$\overrightarrow{\mathbf{V}}_{\mathbf{y}} = \mathbf{A}\,\overrightarrow{\mathbf{V}}_{\mathbf{x}}\,\mathbf{A}^{H}$ $\overrightarrow{\mathbf{m}}_{\mathbf{y}} = \mathbf{A}\,\overrightarrow{\mathbf{m}}_{\mathbf{x}}$	(58) (59)
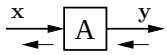	$\overleftarrow{\mathbf{W}}_{\mathbf{x}} = \mathbf{A}^{H}\,\overleftarrow{\mathbf{W}}_{\mathbf{y}}\,\mathbf{A}$ $\overleftarrow{\mathbf{W}}_{\mathbf{x}}\,\overleftarrow{\mathbf{m}}_{\mathbf{x}} = \mathbf{A}^{H}\,\overleftarrow{\mathbf{W}}_{\mathbf{y}}\,\overleftarrow{\mathbf{m}}_{\mathbf{y}}$	(60) (61)

TABLE II: GMP Rules for Composite Blocks with Reduced Computation

Blocks	GMP Rules	
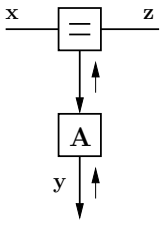	$\overrightarrow{\mathbf{V}}_{\mathbf{z}} = \overrightarrow{\mathbf{V}}_{\mathbf{x}} - \overrightarrow{\mathbf{V}}_{\mathbf{x}}\mathbf{A}^{H}\mathbf{B}\mathbf{A}\overrightarrow{\mathbf{V}}_{\mathbf{x}}$ $\overrightarrow{\mathbf{m}}_{\mathbf{z}} = \overrightarrow{\mathbf{m}}_{\mathbf{x}} + \overrightarrow{\mathbf{V}}_{\mathbf{x}}\mathbf{A}^{H}\mathbf{B}(\mathbf{m}_{\mathbf{y}}^{\uparrow} - \mathbf{A}\overrightarrow{\mathbf{m}}_{\mathbf{x}})$ where $\mathbf{B} = (\mathbf{V}_{\mathbf{y}}^{\uparrow} + \mathbf{A}\overrightarrow{\mathbf{V}}_{\mathbf{x}}\mathbf{A}^{H})^{-1}$	(62) (63) (64)
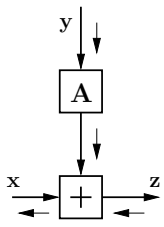	$\overleftarrow{\mathbf{W}}_{\mathbf{x}} = \overleftarrow{\mathbf{W}}_{\mathbf{z}} - \overleftarrow{\mathbf{W}}_{\mathbf{z}}\mathbf{A}\mathbf{C}\mathbf{A}^{H}\overleftarrow{\mathbf{W}}_{\mathbf{z}}$ $\overleftarrow{\mathbf{W}}_{\mathbf{x}}\overleftarrow{\mathbf{m}}_{\mathbf{x}} = (\mathbf{I} - \overleftarrow{\mathbf{W}}_{\mathbf{z}}\mathbf{A}\mathbf{C}\mathbf{A}^{H})*$ $(\overleftarrow{\mathbf{W}}_{\mathbf{z}}\overleftarrow{\mathbf{m}}_{\mathbf{z}} - \overleftarrow{\mathbf{W}}_{\mathbf{z}}\mathbf{A}\mathbf{m}_{\mathbf{y}}^{\downarrow})$ where $\mathbf{C} = (\mathbf{W}_{\mathbf{y}}^{\downarrow} + \mathbf{A}^{H}\overleftarrow{\mathbf{W}}_{\mathbf{z}}\mathbf{A})^{-1}$	(65) (66) (67)

[2] F. Pancaldi, G. Vitetta, R. Kalbasi, N. Al-Dhahir, M. Uysal, and H. Mheidat, "Single-carrier frequency domain equalization," *Signal Processing Magazine, IEEE*, vol. 25, no. 5, pp. 37–56, September 2008.

[3] D. Falconer, S. Ariyavisitakul, A. Benyamin-Seeyar, and B. Eidson, "Frequency domain equalization for single-carrier broadband wireless systems," *Communications Magazine, IEEE*, vol. 40, no. 4, pp. 58–66, Apr 2002.

[4] X. Yuan, Q. Guo, and L. Ping, "Low-complexity iterative detection in multi-user MIMO ISI channels," *Signal Processing*

Letters, IEEE, vol. 15, pp. 25–28, 2008.

[5] H.-A. Loeliger, "Least squares and Kalman filtering on Forney graphs," in *Codes, Graphs, and Systems*, ser. The Kluwer International Series in Engineering and Computer Science, R. Blahut and R. Koetter, Eds. Springer US, 2002, vol. 670, pp. 113–135.

[6] ——, "An introduction to factor graphs," *Signal Processing Magazine, IEEE*, vol. 21, no. 1, pp. 28 – 41, Oca. 2004.

[7] H.-A. Loeliger, J. Hu, S. Korl, Q. Guo, and L. Ping, "Gaussian Message Passing on linear models: An update," in *Turbo Codes Related Topics; 6th International ITG-Conference on Source and Channel Coding (TURBOCODING), 2006 4th International Symposium on*, 2006, pp. 1–7.

[8] H.-A. Loeliger, J. Dauwels, J. Hu, S. Korl, L. Ping, and F. Kschischang, "The factor graph approach to model-based signal processing," *Proceedings of the IEEE*, vol. 95, no. 6, pp. 1295–1322, 2007.

[9] S. Korl, "A factor graph approach to signal modelling, system identification and filtering," Ph.D. dissertation, Swiss Federal Institude of Technology, Zürich, Sweeden, 2005.

[10] R. Drost and A. Singer, "Factor-graph algorithms for equalization," *Signal Processing, IEEE Transactions on*, vol. 55, no. 5, pp. 2052–2065, May 2007.

[11] G. Colavolpe and G. Germi, "On the application of factor graphs and the sum-product algorithm to ISI channels," *Communications, IEEE Transactions on*, vol. 53, no. 5, pp. 818–825, May 2005.

[12] M. Kaynak, T. Duman, and E. Kurtas, "Belief propagation over SISO/MIMO frequency selective fading channels," *Wireless Communications, IEEE Transactions on*, vol. 6, no. 6, pp. 2001–2005, June 2007.

[13] S. Roy and T. Duman, "Soft input soft output Kalman equalizer for MIMO frequency selective fading channels," *Wireless Communications, IEEE Transactions on*, vol. 6, no. 2, pp. 506–514, Feb 2007.

[14] M. Tüchler, A. Singer, and R. Koetter, "Minimum mean squared error equalization using a priori information," *Signal Processing, IEEE Transactions on*, vol. 50, no. 3, pp. 673–683, Mar 2002.

[15] G. Colavolpe, D. Fertonani, and A. Piemontese, "SISO detection over linear channels with linear complexity in the number of interferers," *Selected Topics in Signal Processing, IEEE Journal of*, vol. 5, no. 8, pp. 1475–1485, Dec 2011.

[16] W. Haselmayr, B. Etzlinger, and A. Springer, "Equalization of MIMO-ISI channels based on Gaussian message passing in factor graphs," in *Turbo Codes and Iterative Information Processing (ISTC), 2012 7th International Symposium on*, Aug 2012, pp. 76–80.

[17] Q. Guo and L. Ping, "LMMSE turbo equalization based on factor graphs," *Selected Areas in Communications, IEEE Journal on*, vol. 26, no. 2, pp. 311–319, 2008.

[18] B. Etzlinger, W. Haselmayr, and A. Springer, "Equalization algorithms for MIMO communication systems based on factor graphs," in *Communications (ICC), 2011 IEEE International Conference on*, June 2011, pp. 1–5.

[19] X. Wang and H. Poor, "Iterative (turbo) soft interference cancellation and decoding for coded CDMA," *Communications, IEEE Transactions on*, vol. 47, no. 7, pp. 1046–1061, 1999.

[20] M. Tüchler, R. Koetter, and A. Singer, "Turbo equalization: principles and new results," *Communications, IEEE Transactions on*, vol. 50, no. 5, pp. 754–767, 2002.

[21] L. Liu, W. K. Leung, and L. Ping, "Simple iterative chip-by-chip multiuser detection for CDMA systems," in *Vehicular Technology Conference, 2003. VTC 2003-Spring. The 57th IEEE Semiannual*, vol. 3, April 2003, pp. 2157–2161 vol.3.

[22] Q. Guo and D. Huang, "A concise representation for the soft-in soft-out LMMSE detector," *IEEE Commun. Lett.*, vol. 15, no. 5, pp. 566 –568, May. 2011.

[23] P. Sen, T. Aktas, and A. Yilmaz, "A low-complexity graph-based LMMSE receiver designed for colored noise induced by FTN-signaling," in *Wireless Communications and Networking Conference (WCNC), 2014 IEEE*, April 2014.

[24] J. R. Barry, E. A. Lee, and D. G. Messerschmitt, *Digital Communications*. Springer, 2004.

[25] C. R. Johnson, *Matrix theory and applications*. American Mathematical Soc., 1990, vol. 40.

[26] D. Bertsekas and J. Tsitsiklis, *Introduction to Probability*, ser. Athena Scientific books. Athena Scientific, 2002.

[27] X. Li and J. A. Ritcey, "Bit-interleaved coded modulation with iterative decoding," *Communications Letters, IEEE*, vol. 1, no. 6, pp. 169–171, 1997.

[28] J. Ritcey, "Bit-interleaved coded modulation with iterative decoding using soft feedback," *Electronics Letters*, vol. 34, no. 10, pp. 942–943, May 1998.

[29] M. Tüchler, "Convergence prediction for iterative decoding of threefold concatenated systems," in *Global Telecommunications Conference, 2002. GLOBECOM 2002. IEEE*, vol. 2, Nov 2002, pp. 1358–1362 vol.2.

[30] D. Divsalar, S. Dolinar, and F. Pollara, "Iterative turbo decoder analysis based on density evolution," *Selected Areas in Communications, IEEE Journal on*, vol. 19, no. 5, pp. 891–907, 2001.

[31] S. ten Brink, "Convergence behavior of iteratively decoded parallel concatenated codes," *Communications, IEEE Transactions on*, vol. 49, no. 10, pp. 1727–1737, Oct 2001.

[32] A. Prlja and J. Anderson, "Reduced-complexity receivers for strongly narrowband intersymbol interference introduced by faster-than-Nyquist signaling," *Communications, IEEE Transactions on*, vol. 60, no. 9, pp. 2591–2601, September 2012.

[33] D. Fertonani, A. Barbieri, and G. Colavolpe, "Reduced-complexity BCJR algorithm for turbo equalization," *Communications, IEEE Transactions on*, vol. 55, no. 12, pp. 2279–2287, Dec 2007.

[34] S. M. Kay, *Fundamentals of Statistical Signal Processing: Estimation Theory*. Prentice-Hall, Inc., 1993.